J Mater Sci (2009) 44:6654–6662
DOI 10.1007/s10853-009-3631-4

MESOSTRUCTURED MATERIALS

Total oxidation of volatile organic compounds on Au/Ce–Ti–O and Au/Ce–Ti–Zr–O mesoporous catalysts

C. Gennequin · M. Lamallem · R. Cousin · S. Siffert · V. Idakiev · T. Tabakova · A. Aboukaïs · B. L. Su

Received: 29 November 2008 / Accepted: 19 May 2009 / Published online: 9 June 2009

Abstract Cerium–titanium mixed oxides and mesoporous cerium-modified titanium and cerium-modified titanium–zirconium mixed oxides were synthesized in order to obtain active support for gold volatile organic compound (VOC) oxidation catalysts. Ce–Ti mixed oxides were synthesized by sol–gel method. Mesoporous TiO_2 and Ti–Zr mixed oxides were prepared through the surfactant templating technique. Gold was loaded on supports by deposition-precipitation method. The catalysts were characterized by thermal analysis, XRD, N_2 analysis, TPR, DR/UV–vis and IR. The results evidenced the beneficial role of ceria modifying additive in decreasing the degree of crystallinity of mesoporous support and its particle size. A high degree of synergistic interaction between ceria and mesoporous oxide was observed. H_2-TPR revealed that the reducibility of the catalysts is greatly enhanced in the presence of gold. Considering the light off temperature, the activity of Au/mesoporous cerium-modified titanium oxide is particularly interesting for VOC oxidation comparatively to the same catalysts with a classical support. The gold particles would be more dispersed and stable. However, the sample Au/mesoporous cerium-modified titanium–zirconium mixed oxide is less interesting for VOC oxidation, particularly for toluene oxidation whose activity depends essentially on the adsorption of toluene molecule.

C. Gennequin · M. Lamallem · R. Cousin · S. Siffert (✉) · A. Aboukaïs
Laboratoire de Catalyse et Environnement, E.A. 2598, MREI, Université du Littoral Côte d'Opale, 145 Avenue Maurice Schumann, 59140 Dunkerque, France
e-mail: siffert@univ-littoral.fr

V. Idakiev · T. Tabakova
Institute of Catalysis, Bulgarian Academy of Sciences, 1113 Sofia, Bulgaria

B. L. Su
Laboratory of Inorganic Materials Chemistry, University of Namur (FUNDP), 5000 Namur, Belgium

Introduction

Volatile organic compounds (VOCs) are recognized as major contributors to air pollution, either directly, through their toxic or malodorous nature, or indirectly, as ozone precursors. Many VOC are health hazards in themselves and can cause cancer or other serious illnesses, even at low concentrations. Industrial processes and transportation activities are mainly responsible for the VOC emissions. Technologies for the removal of VOC from gas streams can be broadly classified into two groups: those that recover the VOC for possible later reuse and those that destroy the VOC [1]. Catalytic oxidation of VOC is a chemical oxidation process in which hydrocarbons are combined with oxygen at specific temperatures to yield carbon dioxide and water and it is one of the methods of controlling VOC emissions. Catalytic oxidation is generally preferred to thermal combustion due to the lower temperature required and to its higher selectivity [2].

Gold has been until recently considered as one of the least catalytically useful metals because of its chemical inertness. However, in the last decade it has been widely proved that it is possible to prepare gold nanoparticles deposited on metal oxide supports [3] which exhibit high catalytic activity toward oxidation reactions [4–13]. Supported gold catalyst on titania is often studied since its efficiency for the CO oxidation at low temperature is evidenced [4–10]. Moreover, gold supported on cerium oxide

has been shown to possess high activity for VOC oxidation [14]. Ceria has been widely used in catalysis to purify vehicle exhausts and becomes the most rare earth oxide for controlling pollutant emission. It is known that ceria increases the dispersion of active components. Its most important property is to serve as an oxygen reservoir which stores and releases oxygen via the redox shift between Ce^{4+} and Ce^{3+} under oxidizing and reducing conditions. The Ce^{3+}/Ce^{4+} redox cycle leads to high catalytic activity of ceria catalysts [15–17]. However, since single CeO_2 would be sintered after calcinations at 750 °C, some mixed oxides are prepared by adding anti sintered oxides like titanium [18, 19]. Thus, it should be interesting to combine the physicochemical properties of gold, titanium and cerium in order to obtain a suitable catalytic material for the total oxidation of VOC. However, it was found that the support nature plays an important role in improvement of the efficiency of the catalyst, particularly in oxidation reactions [20–23]. Indeed, recently many nanostructured mesoporous oxides with high surface area and uniform pore size distribution are used as support for multiple catalyst applications [24, 25]. For example, nanostructured mesoporous zirconia and titania supports for vanadia and gold catalysts have provided excellent catalytic properties for complete benzene oxidation [24]. Practical approaches require the preparation of mesoporous materials having hierarchical porous structures at different length scales in order to achieve highly organized functions [26], since hierarchical materials with multiple-scaled porosity can be expected to combine reduced resistance to diffusion and high surface areas for yielding improved overall reaction and adsorption/separation performances. However, the recent conception of new hierarchically metal oxide porous structures lead to a new kind of catalyst supports. These new structures should be able to efficiently transport guest species inside their framework because of their interconnected multimodal porous structure. Moreover, their high surface areas and porous volumes are assets to improve plenty of catalytic reactions and adsorption/separation performance.

The aim of this study is to obtain active catalysts for VOC oxidation. Different preparation routes (classical and for mesoporous) are used for the synthesis of cerium–titanium (Ce–Ti) and cerium–titanium–zirconium (Ce–Ti–Zr) mixed oxides as supports of gold catalysts. These compounds are characterized by XRD, BET surface area, nitrogen adsorption isotherms, TPR, DR/UV–vis and IR and compared catalytically in oxidation of propene and toluene. These molecules are chosen as probe molecules because they are often found in industrial exhausts and present high Photochemical Ozone Creation Potential (POCP) [27].

Experimental

Preparation of mixed oxides Ce–Ti–O

Ce–Ti oxide samples were prepared by a sol–gel method [19]. An aqueous solution of cerium nitrate $Ce(NO_3)_3$, $6H_2O$ and ethanol CH_3CH_2OH were added under stirring to another solution of ethanol CH_3CH_2OH and titanium (IV) isopropoxide $Ti(OC_3H_7)_4$ with molar ratio $Ti(OC_3H_7)_4/CH_3CH_2OH = 1/2$. The molar ratio between H_2O and titanium (IV) precursor is the same that for the titanium oxide preparation. The solution was gelled after finishing the reaction between titanium (IV) isopropoxide $Ti(OC_3H_7)_4$ and water. The gel was dried at 80 °C during 24 h and finally calcined under air for 4 h at 600 °C to obtain $Ce_{0.3}Ti_{0.7}O_2$ called CeTi.

Ce–Ti and Ce–Ti–Zr mesoporous materials preparation

The mesoporous titania was synthesized using surfactant [$C_{13}(EO)_6$–polyoxyethylene(6) tridecylether] templating method through a neutral [$C_{13}(EO)_6$–$Ti(OC_3H_7)_4$] assembly pathway as previously described [24]. The hydrothermal treatment was performed during 48 h at 60 °C. The template was completely removed after 48 h of ethanol extraction.

The preparations of the meso-macroporous materials are processed by the method described elsewhere [26]. The meso-macroporous mixed oxide (TiO_2-ZrO_2) was synthesized as follows: a micellar solution (15 wt%) of decaoxyethylenecetyl ether ($C_{16}(EO)_{10}$) was prepared by dissolving the surfactant at room temperature in an aqueous solution for 3 h. A mixture containing 0.05 mol of zirconium *n*-propoxide ([$Zr(OC_3H_7)_4$], 70 wt% in 1-propanol) and 0.05 mol of titanium propoxide was added drop wise to the above medium. The obtained mixture was then transferred into a Teflon-lined autoclave and heated under static conditions at 60 °C for 48 h. The product was filtered and washed by Soxhlet extraction over ethanol. All mesoporous samples were dried under vacuum at 80 °C and calcined in air at 400 °C for 2 h.

Ceria was loaded on mesoporous titania and meso-macroporous mixed oxide (TiO_2-ZrO_2) by deposition precipitation (DP) method. Before deposition, the mesoporous material was suspended in water by ultrasound technique. Ceria was deposited by precipitation of $Ce(NO_3)_3$,$6H_2O$ with Na_2CO_3 at 60 °C and pH 9.0. The samples were dried under vacuum at 80 °C and calcined in air at 400 °C during 2 h. Ceria modifying additive is 20 wt%. The samples were labeled as CeMTi and CeMTiZr.

Preparation of gold-containing catalysts

The gold-based catalysts were prepared by deposition-precipitation method (DP). Urea was used as precipitating agent for synthesis of $Au/Ce_{0.3}Ti_{0.7}O_2$ (labelled as Au/CeTi) [15]. Aqueous solution of tetrachloroauric acid ($HAuCl_4$) was added under stirring to an aqueous suspension of oxide support CeTi calcined at 600 °C and aqueous solution of urea in excess. The solution was heated at 80 °C to decompose urea and obtain pH equal to 6.7. The pH of solution was maintained at the value of 6.7 during 4 h to obtain high dispersion of fine gold particles on the oxide supports. The mixture was filtered and washed with deionized water at 60 °C several times in order to eliminate the chloride ions, dried during 24 h at 80 °C and finally calcined under air for 4 h at 400 °C.

Deposition of gold hydroxide on mesoporous supports preliminary suspended in water was carried out via chemical reaction between $HAuCl_4 \cdot 3H_2O$ and Na_2CO_3 in aqueous solution. The precipitates were aged for 1 h at 60 °C, filtered and washed carefully until absence of Cl^- ions. The samples were dried under vacuum at 80 °C and calcined in air at 400 °C for 2 h. The catalysts were denoted as Au/CeMTi and Au/CeMTiZr for the samples prepared on ceria-modified mesoporous titania and on ceria-modified meso-macroporous mixed oxide support, respectively.

Sample characterization

To determine the elemental composition of samples, chemical analysis of Ce, Ti and Au was performed by inductively coupled plasma atomic emission spectroscopy at the CNRS Centre of Chemical Analysis (Vernaison, France).

BET surface area was measured by nitrogen adsorption at −196 °C in a Thermo-Electron QSurf M1 apparatus. Before analysis, the samples were degassed for 30 min at 120 °C.

XRD analysis was performed on a BRUKER Advance D8 powder X-ray diffractometer using Cu Kα radiation ($\lambda = 0.15406$ nm). Diffraction patterns were recorded over a 2θ range of 15–85° and using a step size of 0.02° and a step time of 4 s. The mean crystallite sizes were estimated using the Scherrer equation.

The temperature programmed reduction experiments were carried out in an Altamira AMI-200 apparatus. The TPR profiles are obtained by passing a 5% H_2/Ar flow (30 mL/min) through 70 mg of samples heated at 5 °C/min from ambient temperature to 800 °C. The hydrogen concentration in the effluent was continuously monitored by a thermoconductivity detector (TCD).

Diffuse Reflectance UV–visible spectroscopy (DR/UV–vis) experiments were carried out on a VARIAN CARY 5000. The measurements were performed on air exposed samples at ambient temperature between 200 and 800 nm.

Nitrogen adsorption–desorption isotherms were obtained on a Micromeritics TRISTAR 3000 analyzer at −196 °C over a wide relative pressure range from 0.01 to 0.995. The samples were degassed under vacuum for several hours before nitrogen adsorption measurements. The pore diameter and the pore size distribution were determined by the Barret–Joyner–Halenda (BJH) method using the adsorption branch of isotherms.

Toluene oxidation was carried out with operando diffuse reflectance infrared Fourier transform spectroscopy (same conditions as the catalytic tests, part 2.5) on a Brüker Equinox 55 apparatus.

Catalytic activity measurements

Catalytic tests were carried out at atmospheric pressure in a continuous flow tubular glass reactor with an internal catalyst bed. A 100 mg quantity of the catalyst was loaded in the form of fine powder. The gas flow (100 NmL/min with 6000 ppm propene in air or with 1000 ppm of gaseous toluene) was controlled by mass flow controllers. The analysis of combustion products is performed evaluating the propene or toluene conversion and the CO/($CO + CO_2$) molar ratio from a VARIAN CP 4900 μGC. Before the catalytic test, the catalyst (100 mg) is calcined under a flow of air (2 L h^{-1}) at 400 °C (1 °C °min^{-1}).

Results and discussion

Classical Ce–Ti–O and gold deposited on Ce–Ti–O

The textural properties and gold content of the obtained samples are listed in Table 1. A slight decrease in surface area was observed by BET measurement when gold is deposited on the support $Ce_{0.3}Ti_{0.7}O_2$ (CeTi). XRD patterns of the CeTi and Au/CeTi catalysts are reported in Fig. 1. This figure shows that all the samples are characterized by the absence of well resolved diffraction peaks of TiO_2 or CeO_2. This indicates that the solids are in a relatively amorphous state. The highly amorphous character of the samples can be also deduced from the high level of noise detected in the patterns. However, some patterns with bad resolution corresponding to anatase and cerianite phase are revealed. This result indicates that some CeO_2 and TiO_2 crystallites are present in the CeTi oxide sample. The same behavior has been observed by Rynkowski et al. [19] in the case of ceria-titania mixed oxides with atomic ratios Ti/Ce = 8/2. Lopez et al. [28] have evidenced the

Table 1 Characteristics of supports and gold catalysts

Sample	Calcination temperature (°C)	Specific surface area (m^2/g)	Pore diameter (nm)	Pore volume (cm^3/g)[a]	Au content (wt%)
CeTi	600	86	–	–	–
Au/CeTi	400	82	–	–	3.30
CeMTi	400	102.8	10.5	0.3260	–
MTi	400	124.7	11	0.4452	–
Au/CeMTi	400	105.8	11.4	0.3288	3.15
CeMTiZr	400	245	2.0	0.2048	–
Au/CeMTiZr	400	233	2.3	0.2395	2.64

[a] Total pore volumes at $p/p_0 = 0.99$

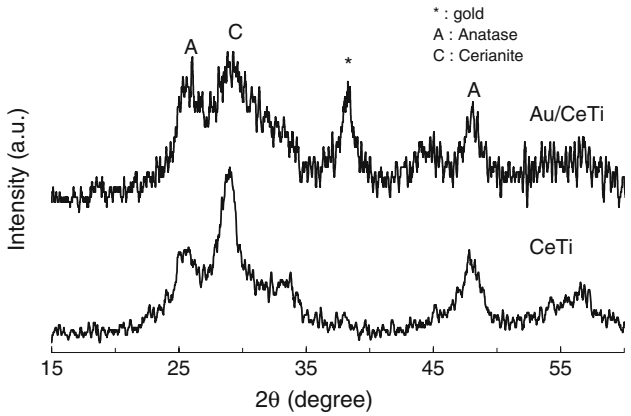

Fig. 1 X-ray diffraction patterns of the ceria-titania support and gold-based catalyst calcined at 400 °C

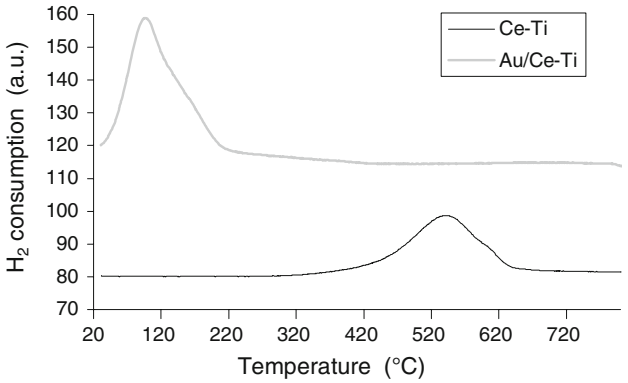

Fig. 2 TPR profiles of the calcined at 600 °C support (Ce–Ti and gold-based catalyst calcined at 400 °C)

appearance of well resolved diffraction lines of cerianite phase in the mixed oxide TiO_2-CeO_2 (90 wt% of TiO_2) after calcination at 800 °C. Those authors have shown that the ceria is formed at low temperature in the form of small dispersed crystallites in the structure of amorphous TiO_2 and which are not detected by the XRD. When increasing the calcination temperature, these crystallites start growing and sintering to constitute larger ones, which allow their detection. No change concerning the structure of the CeTi support due to the gold deposition has been evidenced. However, small diffraction peak at $2\theta = 38.3°$ appears for the sample Au/CeTi. This diffraction pattern corresponds to nanoparticles of metallic gold. The size of the gold particles, deduced from the broadening of this reflexion peak, is evaluated at around 7 nm.

The H_2-TPR profiles of the gold deposited on CeTi presented in Fig. 2 show a reduction peak at low temperature, whereas the TPR profile of the CeTi shows a reduction peak at about 545 °C attributed to the reduction of surface oxygen species from ceria. The peak for Au/CeTi corresponds also to the reduction of the oxygen species on the gold particles and on ceria. Andreeva et al. [29, 30] have showed that adding gold on CeO_2 permits to lower the reduction temperature of oxygen species on ceria surface. This result shows the influence of gold to facilitate the reduction of oxygen species from $Ce_{0.3}Ti_{0.7}O_2$ support surface on the border with gold.

In order to identify the nature of the active gold particles, the CeTi and Au/CeTi catalysts were analyzed by DR/UV–vis spectrometry. The obtained spectra are represented in Fig. 3. Besides support contribution, the UV–vis spectra of the gold-based catalysts show new bands at around 560 and 620 nm. These absorption peaks correspond to metallic gold nanoparticles revealed in previous work [15, 31]. These bands are characteristic of surface plasmon resonance of metallic gold particles which arise from the collective oscillations of the free conduction band electrons that are induced by the incident electromagnetic radiation. Such resonances are observed when the wavelength of the incident light far exceeds the particle diameter.

Mesoporous Ce–Ti–Zr–O and gold deposited on mesoporous Ce–Ti–Zr–O

The XRD patterns of the samples are shown in Fig. 4a and b. The initial mesoporous material shows normal anatase lines (MTi) (Fig. 4a). There are significant differences in the XRD patterns after deposition of ceria additive. The addition of ceria leads to the formation of a defective

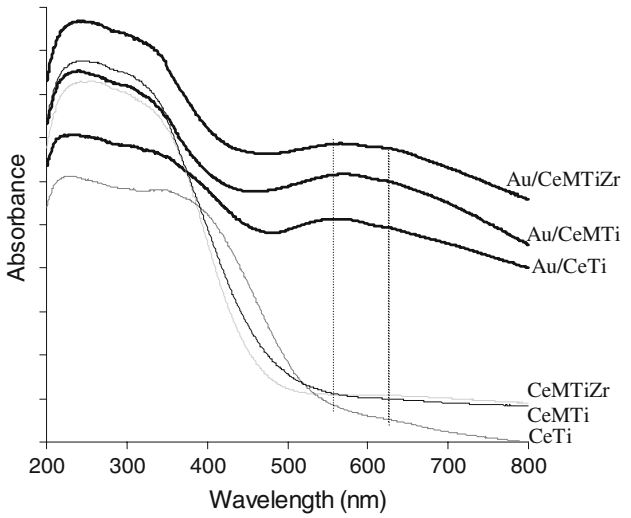

Fig. 3 DR/UV–vis of the oxide supports and gold-based catalysts

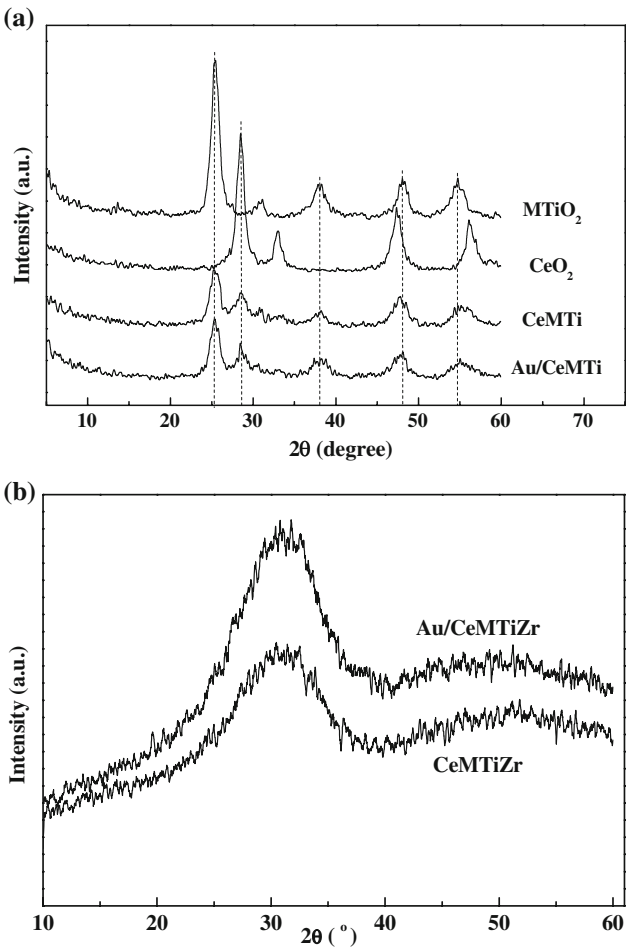

Fig. 4 **a** X-ray diffraction patterns of the ceria-modified mesoporous titania and gold-based catalyst calcined at 400 °C. X-ray diffractograms of $MTiO_2$ and CeO_2 included for clearness. **b** X-ray diffraction patterns of the zirconium-modified mesoporous mixed titanium oxides support and gold-based catalyst calcined at 400 °C

anatase crystal structure (CeMTi). The typical diffraction patterns of anatase are broader and less intensive. No shift of the peak positions ($2\theta = 25.28$, 37.79, 48.04 and 53.88°) can be seen, indicating that no changes in the phase composition occurred. Additionally, no extra lines due to compounds of mixed phases between titania and ceria are registered. Only a weak line at $2\theta = 28.5°$ due to most intense fluorite oxide-type diffraction pattern of CeO_2 is visible. The other diffraction lines, characteristic of cubic structure of ceria ($2\theta = 47.48$ and 56.33°) are not discernible because of their location very close to the respective patterns of titania. The mean particle size of MTi and CeMTi was determinate from XRD line broadening by the Scherrer's equation. The average size of MTi was calculated to be equal to 9.7 nm, while modification by ceria led to its decrease to 6.1 nm. The results revealed the beneficial role of ceria additive in decreasing the degree of crystallinity of MTi and decreasing its particle size. For these mesoporous materials no significant differences after deposition of gold can be detected. The typical lines of gold at $2\theta = 38.2$ and 44.48° in the gold-containing sample calcined at 400 °C (Au/CeMTi) is very hardly observable certainly due to smaller gold nanoparticles on the surface of mesoporous titania and ceria-modified mesoporous titania than on the classical supports.

Moreover, for the DR/UV–vis spectra of Au/CeMTi and Au/CeMTiZr catalysts (Fig. 3), both absorption bands corresponding to gold metallic nanoparticles are detected. Small variations of wavelength of these gold bands are observed which should be induced by the size, the form of crystallites, the surrounding environment and the interaction between gold and support [11, 31–34]. The band centred at 560 nm for Au/CeTi is red shifted to about 575–580 nm for Au/CeMTiZr and Au/CeMTi. This result indicates a decrease in the size of the gold particles [34] according to the XRD data.

The wide-angle XRD patterns of the support (CeMTiZr) and gold-based catalyst (Au/CeMTiZr) are shown in Fig. 4b. No crystalline phase could be detected by XRD in the samples, indicating a homogeneous mixing of the Ti and Zr components in this material. This suggests that the segregation did not occur, and meso-macrostructured TiZr were formed with (Ti,Zr)-O_2 species, a real solid solution of TiO_2 and ZrO_2, rather than discrete TiO_2 and ZrO_2 nanocrystallites. No significant differences after deposition of gold can be detected due also to the very small size of gold particles.

Figure 5 depicts the N_2 adsorption–desorption isotherms (a) and pore size distribution (b) of the supports (MTi and CeMTi) and the gold-based catalyst with different gold contents calcined at 400 °C. The isotherms of all above samples are of type IV, characteristic for mesoporous materials according to the classification of BDDT [35].

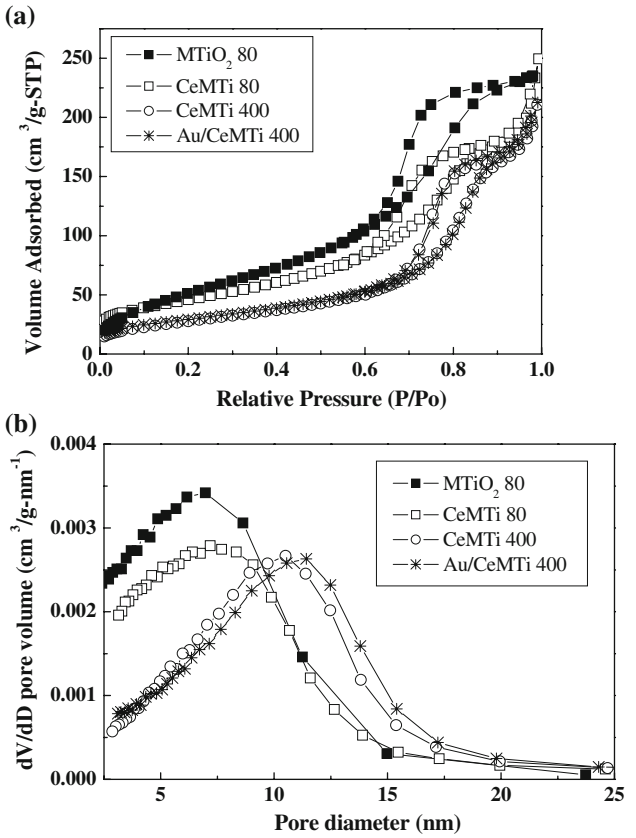

Fig. 5 Nitrogen adsorption isotherms (**a**) and pore size distributions (**b**) of the supports dried at 80 °C and calcined at 400 °C (MTi and CeMTi) and gold-based catalysts supported on CeMTi with different gold content, calcined at 400 °C (Au/CeMTi 400)

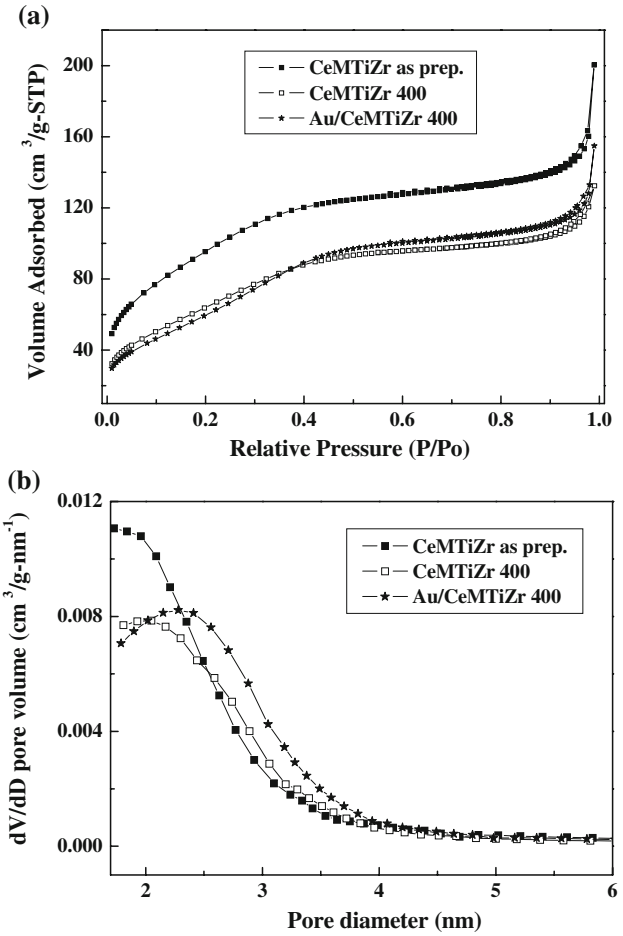

Fig. 6 Nitrogen adsorption isotherms (**a**) and pore size distributions (**b**) of the support CeMTiZr (as prepared and calcined at 400 °C) and gold-based catalyst supported on CeMTiZr calcined at 400 °C (Au/CeMTiZr 400)

A sharp increase in adsorption volume of N_2 is observed in the p/p_0 range of 0.60–0.90, corresponding to the capillary condensation and indicating the good homogeneity of the samples and large pore size since the p/p_0 position of the inflection point is related to the pore size. The pore size distribution obtained with BJH method is quite narrow confirming good quality of our samples. The surface area of mesoporous titania and ceria-modified mesoporous titania are 125 and 103 m^2/g, respectively. After ceria deposition on mesoporous titania, the surface area significantly decreases, as well as the pore volume (Table 1) due very probably to some insertion of the ceria additive into the pores. The differences in the surface areas and pore volumes of support and catalysts with gold loading are insignificant. The pore diameter of gold-loaded catalysts on MTi support remains lower after calcinations compared to pure mesoporous titania, while the gold catalysts supported on CeMTi have practically equal pore diameter (Table 1). The shape of the isotherms and the pore sizes did not change significantly, meaning that material kept its mesoporous structure after introduction of the ceria.

The N_2 adsorption-desorption isotherms (a) and the corresponding BJH pore size distribution curves (b) of the support CeMTiZr and the gold-based catalysts Au/CeMTiZr are shown in Fig. 6. The increase in adsorbed volume at high relative pressure is a direct indication of the presence of the secondary large pores. In general, all samples based on TiZr support exhibit quite narrow pore size distribution peaks, indicative of the homogeneity of the mesoporosity of our materials, with higher surface areas and larger pore volumes. The textural properties of the obtained samples are listed in Table 1. The BET surface area of the calcined support is larger than those of the calcined gold-based catalyst. The decreasing of the value is insignificant, about 5%.

In Fig. 7, the TPR profiles of the supports (MTi and CeMTi) and the gold-based catalyst (Au/CeMTi) as well as that of ceria for comparison are shown. In the profile of mesoporous titania (MTi) only a peak at above 500 °C due to the titania reduction is observed. The modification with

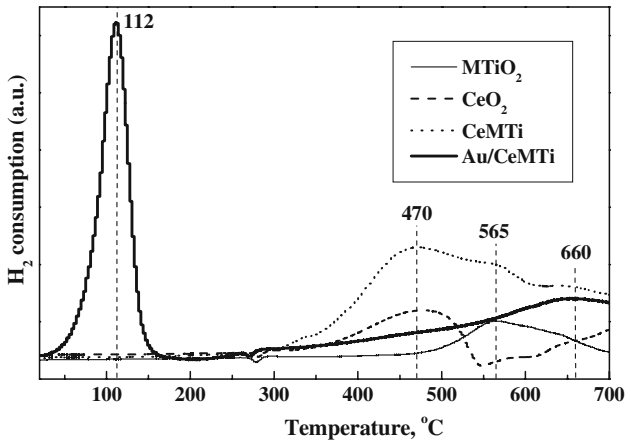

Fig. 7 TPR profiles of the supports calcined at 400 °C ($MTiO_2$, CeO_2, and CeMTi), and gold-based catalyst (Au/CeMTi)

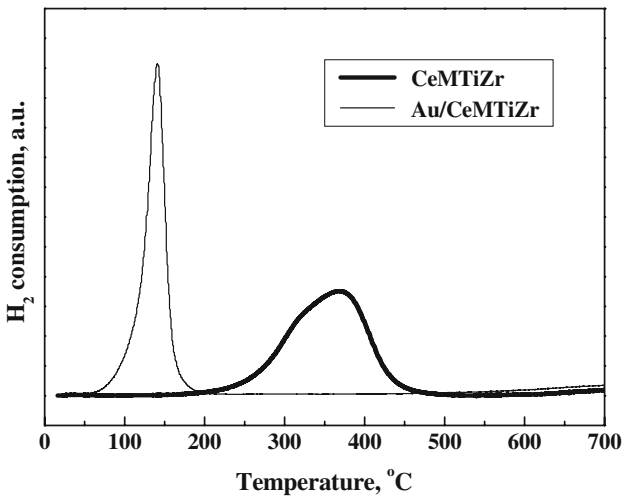

Fig. 8 TPR profiles of the support (CeMTiZr) and gold-based catalyst (Au/CeMTiZr) calcined at 400 °C

ceria causes strong effect on the reducibility of mesoporous titania. Differences are observed both in the intensity and the shape of the TPR peaks. The H_2-TPR profile of ceria contains two major peaks, one at lower temperature (around 500 °C), attributed to the reduction of surface oxygen, and another at higher temperature (around 800 °C), attributed to the removal of bulk oxygen from the ceria structure as reported by Yao and Yao [17]. A significant increase of the intensity of the peak at 470 °C assigned to ceria surface oxygen reduction is registered in the TPR profile of ceria-modified mesoporous titania. This higher hydrogen consumption could be related to the synergistic interaction of ceria and mesoporous titania in agreement with results from the other characterization methods used. Clear evidence that gold facilitates the reducibility of the surface oxygen of ceria-modified mesoporous titania is found by H_2-TPR. An intense and sharp low-temperature (LT) peak with $T_{max} = 112$ °C is observed in the TPR profile of Au/CeMTi. A recent TPR study of Au/ceria catalysts prepared by DP method has shown that the hydrogen consumption at low temperature is due to two processes, namely, the reduction of oxygen species on nanosize gold particles and the surface reduction of ceria [29]. This is in agreement with other studies that the presence of noble metals can increase the oxygen storage capacity of CeO_2 due to noble metal–CeO_2 interaction. Two reduction peaks have been observed in the profile of gold supported mesoporous titania [25]. The low-temperature (LT) peak has been assigned to the reduction of oxygen species on the nanosize gold particles and to the $Ti^{4+} \rightarrow Ti^{3+}$ reduction on the border with gold particles. It was also observed that the addition of gold promotes the formation of superoxide O^{2-} bound to Ti^{4+} and proposed that the presence of Au species make easy the formation of oxygen defects on titania surface at the boundary of gold particles. We can conclude that (i) the ceria additive interacts with the mesoporous titania and induces strong effect on the reducibility of the support; (ii) the gold loading promotes the reducibility of the surface oxygen of ceria-modified mesoporous titania; (iii) the presence of gold and ceria species makes easy the formation of oxygen defects at the boundary of titania surface.

Figure 8 illustrates the TPR profiles of the support (CeMTiZr) and corresponding gold catalyst (Au/CeTiZr). The modification with ceria of meso-macroporous support (TiZr) causes strong effect on its reducibility and the peak appears at 365 °C. Clear evidence that gold facilitates the reducibility of the CeMTiZr support is found by H_2-TPR. An intense and sharp low-temperature (LT) peak with $T_{max} = 80$ °C is observed in the TPR profile of Au/CeMTiZr. The LT peak can be assigned to the reduction of oxygen species on the nanosize gold particles and to the almost fully reduction of the support.

Catalytic total oxidation of toluene and propene

Figure 9 presents the conversion of propene or toluene as function of the temperature in the presence of the different gold-based catalysts. The supports are not sufficiently active to be interesting but the addition of gold on the supports improves the catalytic activity for the VOC oxidation. The VOC (propene or toluene) conversion is then performed at low temperature and present 100% of selectivity toward formation of CO_2. It can be observed that the catalytic activity changes according to the nature of support. It seems that the gold deposited on CeMTi presents the best catalytic activity for the total propene and toluene oxidation and this activity is much higher than the same catalyst with a classical support. The higher gold dispersion can explain this interesting result. However, it can be noticed that the sample Au/CeMZrTi is less efficient than

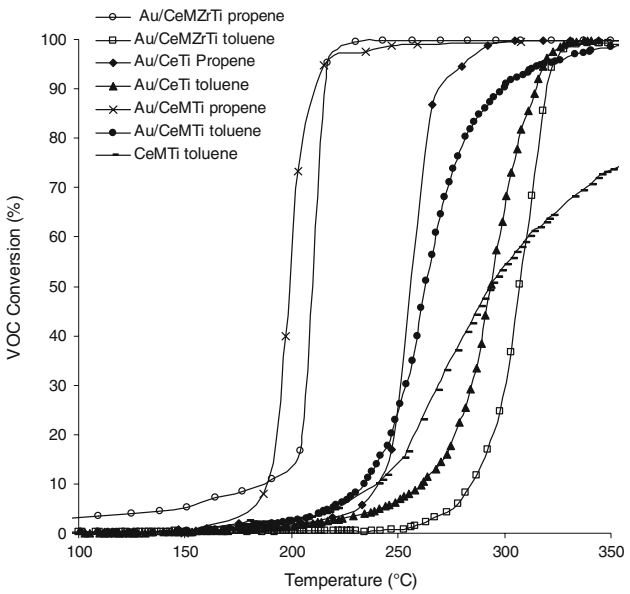

Fig. 9 Propene and toluene conversions versus temperature over gold catalysts

Au/CeMTi. This result could be correlated to H_2-TPR data. This observation could be explained by the interaction between gold nanoparticles and cerium oxide. Ceria is very well known for its oxygen storage capacity (OSC), defined as the capacity to release and accept oxygen. Centeno et al. [7] have studied the catalytic combustion of VOC on Au/CeO_x/Al_2O_3, and they concluded that the presence of cerium ions has a positive influence on the fixation and the final dispersion of gold on alumina support. Moreover, ceria stabilizes the gold particles with low crystallite size. In addition to these beneficial features, ceria, because of its redox properties, may improve the catalytic behavior of the catalyst by increasing the supply of active oxygen. Similar conclusions were proposed by Sciré et al. [14] in their study of VOC oxidation over Au/CeO_2. The mechanism of hydrocarbon oxidation over ceria and other reducible metal oxides is usually considered to be of the redox or Mars and van Krevelen type [7, 14]. The key steps of this mechanism are believed to be the supply of active oxygen by the readily reducible oxide and its reoxidation by oxygen. Gluhoi et al. [36] have shown that gold-based catalysts that contain a transition metal oxide or ceria are highly active in propene oxidation. The role of the oxide is twofold: it stabilizes the gold particles against sintering (ceria) and provides active oxygen for the reaction. Nevertheless, another factor observed by the use of operando DRIFT (not shown) for toluene oxidation can be important for the activity. Thus, the band corresponding to the aromatic C–C bond is higher for Au/CeMTi (1510 cm^{-1}) than for Au/CeMZrTi (1496 cm^{-1}), indicating a higher interaction of toluene on the latter sample which implies a lower activity for toluene oxidation [37]. The incorporation of zirconium in the support seems then to increase the toluene interaction. Moreover, the propene interaction with the catalyst should be less important than for the toluene [38] and thus the sample Au/CeTi is more active than the catalyst Au/CeMZrTi for toluene oxidation.

Conclusion

On the basis of the results reported, we can conclude that mesoporous materials as supports of gold-based catalysts have an important and interesting effect on the VOC oxidation activity.

The ceria additive interacts with the mesoporous supports and induces strong effect on its reducibility. The gold loading significantly promotes the reducibility of ceria-modified metal oxides.

The analysis of the obtained catalytic activity results reveals that Au/CeMTi is promising catalysts for VOC conversion comparatively to the same catalysts with a classical support. It could be suggested a good possibility for practical application of these materials for efficient removal of VOC. The red shift of the UV–vis gold band indicates that the size of the gold particles would be smaller than on the classical support.

However, the sample Au/mesoporous cerium-modified titanium–zirconium mixed oxide is less interesting for VOC oxidation than Au/CeMTi, particularly for toluene oxidation whose activity is correlated to the adsorption of toluene.

Acknowledgements This work was partly supported by IRENI and the "Région Nord - Pas de Calais" through a research grant and by a European INTERREG IV French–Wallonia program.

References

1. Okeke O (1995) Proc. conference VOC's in the environment, London, p 3
2. O'Malley A, Hodnett BK (1999) Catal Today 54:31
3. Ivanova S, Petit C, Pitchon V (2004) Appl Catal A 267:191
4. Bond GC (2002) Catal Today 72:5
5. Grisel RJH, Nieuwenhuys BE (2001) Catal Today 64:69
6. Daté M, Haruta M (2001) J Catal 201:221
7. Centeno MA, Paulis M, Montes M, Odriozola JA (2002) Appl Catal A 234:65
8. Minico S, Sciré S, Crisafulli C, Galvagno S (2001) Appl Catal B 34:277
9. Grundwaldt JD, Maciejewski M, Becker OS, Fabrizioli P, Baiker A (1999) J Catal 186:458
10. Gasior M, Grzybowska B, Samson K, Russel M, Haber J (2004) Catal Today 91–92:131
11. Zanella R, Giorgio S, Shin CH, Henry CR, Louis C (2004) J Catal 222:357
12. Haruta M (2002) CATTECH 6:102

13. Gennequin C, Lamallem M, Cousin R, Siffert S, Aïssi F, Aboukaïs A (2007) Catal Today 122:301
14. Sciré S, Minico S, Crisafulli C, Satriano C, Pistone A (2003) Appl Catal B 40:43
15. Lamallem M, El Ayadi H, Gennequin C, Cousin R, Siffert S, Aïssi F, Aboukaïs A (2008) Catal Today 137:367
16. Otsuka K, Wang Y, Nakamura M (1999) Appl Catal A 183:317
17. Yao HC, Yao YFY (1984) J Catal 86:254
18. Terribile D, Trovarelli A, Llorca J (1998) J Catal 178:299
19. Rynkowski J, Farbotko J, Touroude R, Hilaire L (2000) Appl Catal A 203:335
20. Okumura K, Kobayashi T, Tanaka H, Niwa M (2003) Appl Catal B 44:325
21. Hosseini M, Tidahy LH, Siffert S, Cousin R, Aboukais A, Su BL (2008) SSSC 174:1323
22. Kapoor MP, Ichihashi Y, Shen WJ, Matsumura Y (2001) Catal Lett 76:139
23. Lin W, Lin L, Zhu YX, Xie YC, Scheurell K, Kemnitz E (2005) J Mol Catal A 226:263
24. Idakiev V, Ilieva L, Andreeva D, Blin JL, Gigot L, Su BL (2003) Appl Catal A 243:25
25. Idakiev V, Tabakova T, Yuan ZY, Su BL (2004) Appl Catal A 270:135
26. Yuan ZY, Ren TZ, Vantomme A, Su BL (2004) Chem Mater 16:5096
27. Derwent RG, Jenkin ME, Saunders SM, Pilling MJ (1998) Atmos Environ 32:2429
28. Lopez T, Rojas F, Katez RA, Galindo F, Balankin A, Buljan A (2004) J Sol Stat Chem 177:1873
29. Andreeva D, Idakiev V, Tabakova T, Ilieva L, Falaras P, Bourlinos A, Travlos A (2002) Catal Today 72:51
30. Munteanu G, Ilieva L, Nedyalkova R, Andreeva D (2004) Appl Catal A 277:31
31. Lamallem M, Cousin R, Thomas R, Siffert S, Aïssi F, Aboukaïs A (2009) CR Chimie 12:772
32. Lee Y, Kim D, Shin S, Oh S (2006) Mater Chem Phys 100:85
33. Sun J, Fujita S, Zhao F, Hasegawa M, Arai M (2005) J Catal 230:398
34. Gluhoi AC, Tang X, Marginean P, Nieuwenhuys BE (2006) Top Catal 39:1
35. Brunauer S, Deming LS, Deming WS, Teller E (1970) J Am Chem Soc 62:1723
36. Gluhoi AC, Bogdanchikova N, Nieuwenhuys BE (2005) J Catal 232:96
37. Hosseini M, Siffert S, Cousin R, Aboukaïs A, Hadj-Sadok Z, Su B-L (2009) CR Chimie 12:654
38. Hosseini M, Siffert S, Tidahy HL, Cousin R, Lamonier J-F, Aboukais A, Vantomme A, Roussel M, Su BL (2007) Catal Today 122:391